J. MATER. RES. TECHNOL. 2013;2(1):18-23

jmr&t Journal of Materials Research and Technology
www.jmrt.com.br

Original Article

Processing and characterization of Al_2O_3-yttrium aluminum garnet powders

Eduardo de Souza Lima[a,*], *Luis Henrique Leme Louro*[a], *Ricardo de Freitas Cabral*[b], *José B. de Campos*[c], *Roberto Ribeiro de Avillez*[d], *Célio Albano da Costa*[e]

[a]*Instituto Militar de Engenharia (IME), Rio de Janeiro, RJ, Brazil*
[b]*Universidade Estadual da Zona Oeste (UEZO), Rio de Janeiro, RJ, Brazil*
[c]*Universidade do Estado do Rio de Janeiro (UERJ), Rio de Janeiro, RJ, Brazil*
[d]*Materials Engineering Department, Pontifícia Universidade Católica do Rio de Janeiro (PUC-Rio/DEMa), Rio de Janeiro, RJ, Brazil*
[e]*Instituto Alberto Luiz Coimbra de Pós-Graduação e Pesquisa de Engenharia, Universidade Federal do Rio de Janeiro (COPPE/UFRJ), Rio de Janeiro, RJ, Brazil*

ARTICLE INFO

Article history:
Received 19 August 2012
Accepted 16 October 2012

Keywords:
Al_2O_3-yttrium aluminum garnet composite
Milling
Powders

ABSTRACT

Recent studies have shown that $Y_3Al_5O_{12}$ (YAG - yttrium aluminum garnet) and Al_2O_3 composites are chemically stable at high temperatures when produced by unidirectional solidification. In this method, the material is slowly solidified immediately after passing through a melting zone. However, this complexity procession has encouraged other routes. Among them, the usual sintering of Al_2O_3 and Y_2O_3 (or YAG) powders. In this present work, Al_2O_3 and YAG powders were produced using a high-energy milling of Al_2O_3 and Y_2O_3 precursor powders followed by a thermal treatment step. These powders were characterized using quantitative XRD techniques, BET, SEM and TEM. The complete YAG formation was obtained at 1,400 °C.

1. Introduction

Several studies have revealed [1-8] the potential use of YAG oxides as reinforcing element in an Al_2O_3 ceramic matrix. Both YAG and Al_2O_3 have similar thermal expansion coefficient and they are chemically stable due to their low O_2 vapor pressure. In addition, there is a eutectic reaction at 1826 °C in the Al_2O_3-Y_2O_3 system. It enables a fusion processing, evolving a liquid phase, turning the Al_2O_3-YAG composites very attractive. This eutectic reaction is possible for compositions containing from 18.5 to 20.5 mol% Y_2O_3 [2,9,10].

Although its advantages, the Al_2O_3-YAG eutectic composite fabrication process is extremely complex and its development is restricted to the well-defined eutectic composition. These reasons have led to the investigation of the polycrystalline dual phase Al_2O_3-YAG composite [11,12]. In this study, Al_2O_3 and Y_2O_3 precursors powders have been processed by milling aiming the Al_2O_3-YAG powders composites production. The milling time optimization was determined based on the particle size distribution evaluation and BET. The heat treatment temperature for full YAG formation was carried on by XRD (X-ray Diffraction) combined with Rietveld Method [13] for quantitative phase determination.

*Corresponding author.
E-mail address: eslima@hotmail.com (E.S. Lima).

2238-7854/$ - see front matter http://dx.doi.org/10.1016/j.jmrt.2013.03.005

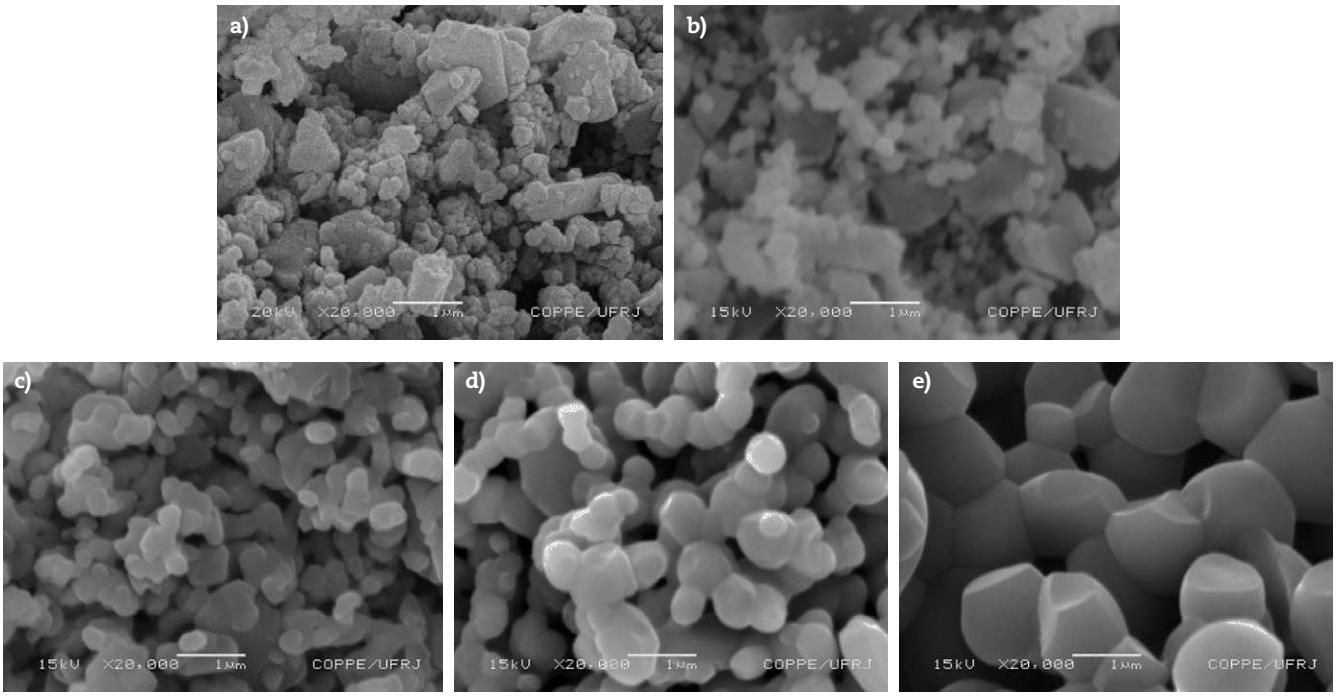

Fig. 1 – (a) Microstructure of the green body; (b) no significant changes were observed at 1,000 °C; (c), (d) and (e) the pellets consisted of a fine particle network surrounded by big voids with extensive necking between particles, whose size increases with temperature, respectively at 1,200 °C, 1,400 °C and 1,600 °C.

2. Methods

Commercially available powders of Y_2O_3 (Alfa Aesar, REO, 99.9%) and Al_2O_3 (Alcoa, APC 2011, 99.7%) with the eutectic Al_2O_3-YAG molar ratio of 20.5:79.5 (or 36.35:63.65 wt%) [2,9,10] were milled in a planetary mill for 2 hours. The slurry was then dried in a furnace at 120 °C for 48 hours. The soft agglomerated powder was then crushed and sieved. Green bodies were uniaxially pressed at 30 MPa. The green pellets were heat treated in air at 1,000 °C, 1,200 °C, 1,400 °C and 1,600 °C during 3 hours. Pellets surface fracture were gold-coated prior to observation in a JEOL JSM-6460LV scanning electron microscope (SEM) using secondary electrons imaging. The pellets were again crushed in a mortar and pestle and the produced powder was milled like before. The powder was observed in a JEOL EM-2010 transmission electron microscope (TEM) with an EDS (Energy Dispersive X-Ray Spectroscopy) Noran System SIX, Model 200. A Cu grid was used for the powders support.

Phase formation characterization was performed using XRD techniques, carried out on these samples using a Panalytical X'PERT PRO diffractometer with CuKα radiation, a scanning step of 0.05° and a collecting time of 5 seconds per step. Quantitative Rietveld calculations [13] were done using Bruker-AXS TOPAS, version 2.1 [14,15] for phase determination. For these calculations, the lattice parameter, the crystalline size and the scale were adjusted and the fraction of crystalline phases determined.

The surface specific area was evaluated both on the as-received and on the processed powders, by means of the BET method using a Micromeritics Gemini 2375. The particle size measurements were performed both on the as-received and on the processed powders by a CILAS (Company Industrielle des Lasers) 1090 laser particle size analyzer.

3. Results and discussion

The initial pellet, made up of Y_2O_3 and Al_2O_3, is shown in Fig. 1a and consists of irregularly shaped particles. The smallest ones are Y_2O_3. No significant changes were observed at 1,000 °C, Fig. 1b. The morphological aspects of heat treated pellets at 1,200 °C, 1,400 °C and 1,600 °C, presented in Figs. 1c, d and e, respectively, revealed that they consisted of a fine particle network surrounded by big voids with extensive necking between particles. The network particle size increased with temperature treatment [16]. In his search, Kong [17] has also found a significant microstructural increase as a function of increasing annealing temperature on this same Al_2O_3-Y_2O_3 system. The grain size increased from 0.3 to 1.5 micrometers as the temperature rose from 1,100 °C to 1,500 °C, respectively [17].

XRD measurements with Rietveld refinements were performed on the samples milled for 120 minutes and heat treated at 1,200 °C and 1,400 °C for qualitative phase evaluation. The Rietveld Method was applied for phase quantification as showed in Figs. 2a to 2c. The Goodness of Fitting (GOF) varied between 1.50 and 2.05 and Rw varied between 13.85 and 26.46. Table 1 shows the phase quantifications depicted on Fig. 2.

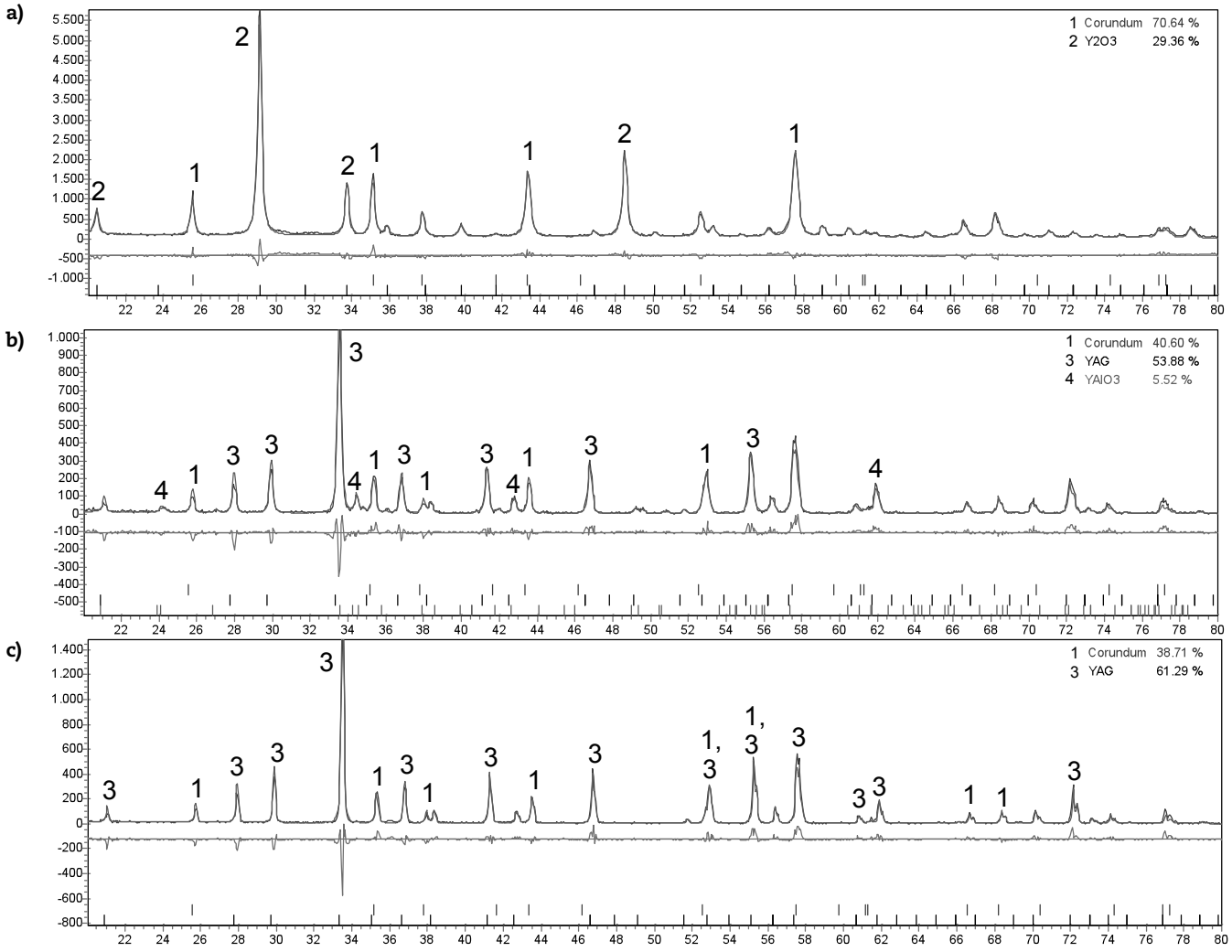

Fig. 2 – Rietveld calculations of the (a) milled powders; (b) 1,200 °C and (c) 1,400 °C. YAG: yttrium aluminum garnet.

The milled powder sample observations confirmed the presence of Al_2O_3 and Y_2O_3 phases. From the quantitative XRD, it was possible to confirm the existence of Al_2O_3 contamination due to the milling balls, as the measured Al_2O_3 concentration was 70.6 wt%, higher than the initial eutectic composition (63.65 wt%).

At 1,200 °C, most YAG was formed with 53.9 wt%, but there was still the presence of an intermediary phase named $YAlO_3$ (YAP – yttrium aluminum perovskite) with 5.5 wt%. At 1,400 °C, the YAP reacted with Al_2O_3 yielding YAG full phase transformation after three hours of heat treatment, with 61.3 wt%, near the expected composite composition, of 63.7 wt% [18].

Table 1 – Rietveld X-ray Diffraction quantitative results (wt. %).

Sample/Phase	Al_2O_3	Y_2O_3	$YAlO_3$	YAG
Al_2O_3-Y_2O_3 (120 min milling time)	70.6	29.4	–	–
1,200 °C heat treated	40.6	–	5.5	53.9
1,400 °C heat treated	38.7	–	–	61.3

According to the literature, regardless of the molar ratio used between the initial Al_2O_3 and Y_2O_3 powders, solid-state reaction develops in three stages [16,19], described by Eqs. (1) to (3):

$$2Y_2O_3 + Al_2O_3 = Y_4Al_2O_9 \text{ (YAM, 900-1,100 °C)} \quad (1)$$

$$Y_4Al_2O_9 + Al_2O_3 = 4YAlO_3 \text{ (YAP, 1,100-1,250 °C)} \quad (2)$$

$$3YAlO_3 + Al_2O_3 = Y_3Al_5O_{12} \text{ (YAG, 1,250-1,600 °C)} \quad (3)$$

Temperatures in parentheses indicate the beginning range of phase formation. The reactions occur by diffusion of O and Al ions toward the other phases. However, the complete transformation demands time, higher temperatures and powders reactivity. The complete YAG formation by solid-state reaction is only possible with heating at 1,600 °C by 20 hours or at 1,700°C [16,19-21].

The lowest temperature of YAG full formation was obtained by co-precipitation method by LI [22], at 800 °C, with 2 hours

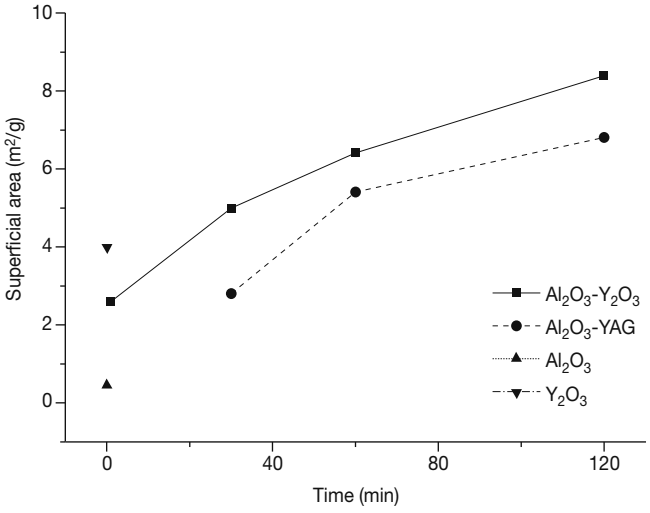

Fig. 3 – BET superficial area variation with milling time of the Al_2O_3-Y_2O_3 mixture.

heat treatment. There was no intermediary phase formation. According to the author, the lowest formation temperature was possible due to the good homogeneity of the reagents, in the order of nanometers.

Wen [19] used a mixed process, with the use of chemical method and the solid state reaction. It was initially produced nanometer Y_2O_3 by the chemical method, which was later joined with powdered commercial Al_2O_3 with 220 nm medium particle size. The YAG was produced by solid state reaction by heating the mixture at 1,300 °C for 2 hours. According to the researcher, a good mix and high dispersion and activity of initial powders were responsible for the low temperature YAG formation in comparison to the solid state reaction method.

This phase comes from a second solid state reaction for YAG formation, where YAP is formed from $Y_4Al_2O_9$ (YAM – yttrium aluminum monoclinic) consumption. The YAM formation can be detected between 950 °C and 1,000°C. The temperature increase above 1,000 °C facilitates the formation of the YAP phase [16,19].

Palmero [23] found an initial amount of YAG at 1,300 °C. However, its complete formation was given only at 1,500 °C.

The ICSD (Inorganic Crystal Structure Database) files used in TOPAS with crystallographic information were: 86817 for Y_2O_3; 93096 for Al_2O_3; 86817 for $YAlO_3$ and 96635 for YAG. This ICSD files contains all crystallographic phase information necessary for Rietveld calculations, as the space group, atomic positions, lattice sites and lattice parameters.

Fig. 3 shows the BET results, for the as-received powders, for the Al_2O_3 and Y_2O_3 (AYO), and for Al_2O_3 and YAG (AYE) mixtures as a function of milling time. The milling process provided a substantial increase of the superficial area which is very important to speed up the sintering step.

Fig. 4a and b shows the particle size evolution of Al_2O_3-Y_2O_3 and Al_2O_3-YAG mixtures with the milling time, where the three curves represents the d_{10}, d_{50} and d_{90} particle size distribution. This notation indicates that 10%, 50% e 90% of the particle volume are below the particle size indicated. The Al_2O_3-Y_2O_3 mixture distribution curve (Fig. 4a) showed an initial substantial decrease of the particle size that leveled off for milling times above 60 min, even though the superficial area (Fig. 3) showed a continuous increase with the milling time. The Al_2O_3-YAG mixture distribution curve (Fig. 4b) showed a constant decrease of the particle size with the milling time. Despite the observed very small reduction of the particle size, the area measured by BET increased with milling time.

It is probable that the smallest particles were bonding by the milling process with a very rough surface that would increase the surface area measured by BET (Fig. 3) without a substantial decrease of particle sizes (Fig. 4). Indeed, Fig. 5 seems to corroborate this process. Fig. 5a has revealed submicron particles with irregular borders and shapes, and particle morphology with different aspect ratios. This latter feature corresponds to the original powder morphology, before milling. It is observed the formation of clusters of submicron

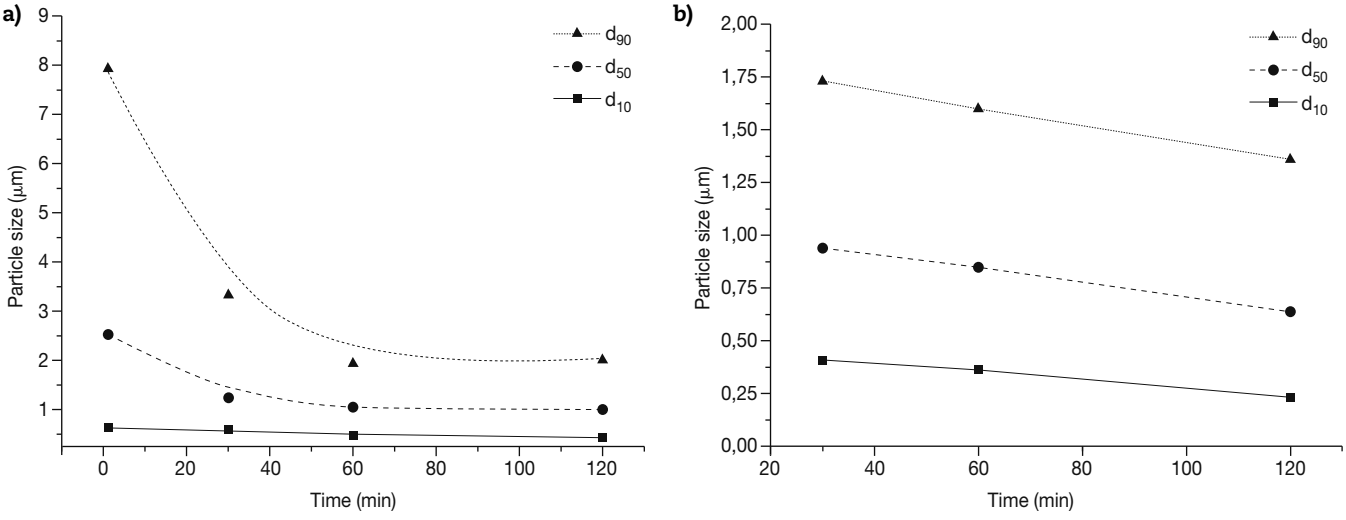

Fig. 4 – d_{10}, d_{50} and d_{90} particle size distribution of (a) Al_2O_3 and Y_2O_3 and (b) Al_2O_3 and yttrium aluminum garnet powders with milling time.

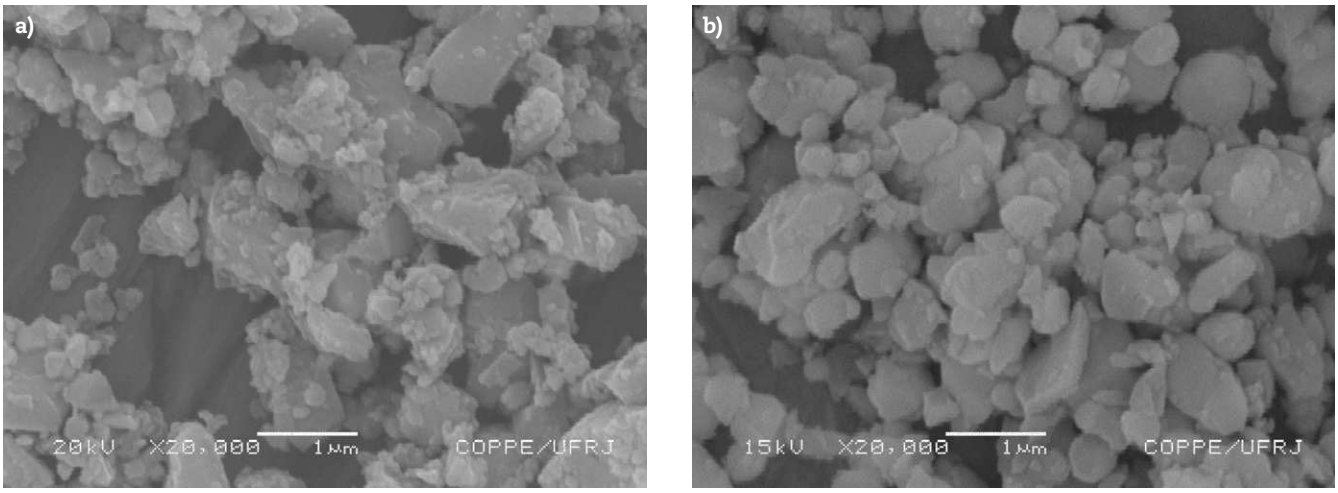

Fig. 5 – Scanning electron microscope secondary electron, 20,000× magnification of (a) Al_2O_3-Y_2O_3 mixture milled for 120 min; (b) Al_2O_3-yttrium aluminum garnet mixture milled for 120 min.

particles which can lead to the important difference between the results of the particle size and the superficial area analysis. Fig. 5b shows submicron particles with less irregular and round borders as well as aspect ratio near to one, but also with clusters of particles.

Figs. 6a and 6b show Al_2O_3-YAG composite particles with 120 min. milling time on TEM, under 40,000 and 80,000× magnification. The presented process resulted in a powder with a complex morphology, consisting of softly agglomerated submicrometer irregular shapes.

This figure also presents the EDS spectrum from the numbered particles. The analysis pointed that particle 1 consists of Al and O, which probably indicates an Al_2O_3 particle. The other particles, 2, 3 and 4, consist of Al, O and Y, which may identify YAG particles. The source of Cu in the EDS spectrums corresponds to the holder.

The morphology did not allow establishing differences among the particles. Nevertheless, the absence of phase contrast and the EDS results corroborates the conclusion that the particles are homogeneous and distinct. Other studies have reported softly agglomerated, submicrometer and distinct particles of Al_2O_3 and YAG in the YAG or Al_2O_3-YAG powder production by other methods: a ball-mill technique in an aqueous medium [24], a co-precipitation method [3] and an aqueous sol-gel method [25].

4. Conclusions

The results revealed that the YAG was fully formed from a mixture of Al_2O_3 and Y_2O_3 milled for 2 hours and heat treated after 1,400 °C for 3 hours. The proposed process provides a much lower temperature for the YAG formation compared with the minimum of 1,600 °C reported in the literature for normal grain size raw materials.

The particle size studies of the Al_2O_3-YAG milled powders were able to determine the optimal milling time around 120 min. The formation of agglomerated submicron Y_2O_3 particles leads to important differences between the results of the particle size and the superficial area analysis. X-ray characterization revealed the presence of an intermediate

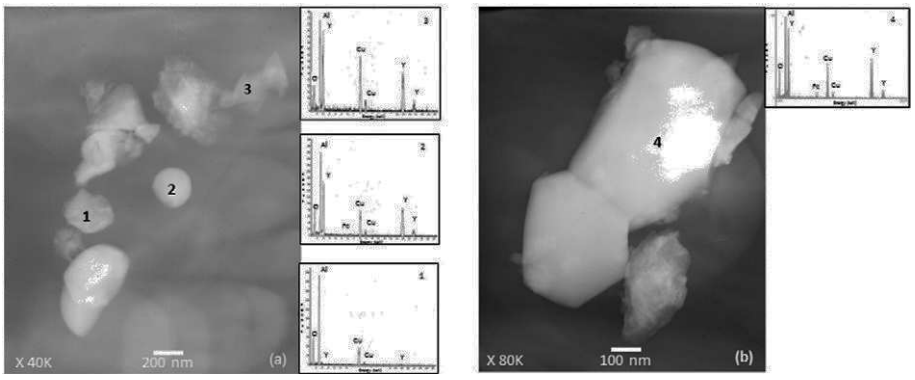

Fig. 6 – (a) and (b): Transmission electron microscope micrographs and Energy Dispersive X-Ray Spectroscopy of Al_2O_3 and yttrium aluminum garnet particles.

phase, $YAlO_3$, for heat treatment at 1,200 °C, which was observed in previous studies [12,18].

The quantitative XRD with Rietveld calculations revealed Al_2O_3 contamination in the composite powder, which changed the stoichiometry of the initial solid-state reaction. It was not possible to establish the initial temperature for the formation of YAG, but at 1,200 °C it had already a major amount compared to the $YAlO_3$ phase.

Further studies are on the way, where the full transformation temperature will be evaluated with sharper step range. Also the phase formation kinetics will be investigated for processing optimization with the characterization of the possible intermediary phases like $YAlO_3$ and $Y_4Al_2O_9$, as described before [15,18].

The presented process resulted in an Al_2O_3 and YAG powders with a complex morphology, consisting of a softly agglomerated submicrometer irregular shapes.

Acknowledgements

The authors would like to thanks: E.S. Lima the support of IEN in the BET measurements; J.B. de Campos the support of MCT; R.R. de Avillez acknowledges the support of CNPq.

REFERENCES

[1] Ochiai S, Ueda T, Sato K, et al. Deformation and fracture behavior of an Al_2O_3/YAG composite from room temperature to 2023 K. Compos Sci Technol. 2001;61:2117-28.

[2] Waku Y, Nakagawa N, Wakamoto T, Otsubo H, Shimizu K, Kohtoku Y. High temperature strength and thermal stability of unidirectionally solidified Al_2O_3/YAG eutectic composite. J Mater Sci. 1998;33:1217-25.

[3] Palmero P, Simone A, Esnouf C, Fantozzi G, Montannaro L. Comparison among different sintering routes for preparing alumina-YAG nanocomposites. J Eur Ceram Soc. 2006;26: 941-7.

[4] Li W, Gao L. Processing, microstructure and mechanical properties of 25 vol% YAG-Al_2O_3 nanocomposites. Nanostruct Mater. 1999;11:1073-80.

[5] Parthasarathy TA, Mah T, Matson LE. Processing, structure and properties of alumina-YAG eutectic composites. J Ceram Process Res. 2004;5:380-90.

[6] Ochiai S, Sakai Y. Analytical modeling of stress-strain behavior at 1873 K of alumina/YAG composite compressed parallel and perpendicular to the solidification direction. Compos Sci Technol. 2006;(66):1-8.

[7] Pastor J, Llorca Y, Salazar A. Mechanical properties of melt-grown alumina-yttrium aluminum garnet eutectics up to 1900 K. J Am Ceram Soc. 2005;88:1488-95.

[8] Ochiai S, Sakai Y. Fracture characteristics of Al_2O_3/YAG composite at room temperature to 2023 K. J Eur Ceram Soc. 2005;25:1241-9.

[9] Mizutani Y, Yasuda H, Ohnaka I, Maeda N, Waku Y. Coupled growth of unidirectionally solidified Al_2O_3–YAG eutectic ceramics. J Cryst Growth. 2002;244:384-92.

[10] Isobe T, Omori M, Uchida S, Sato T, Hirai T. Consolidation of Al_2O_3-$Y_3Al_5O_{12}$ (YAG) eutectic powder prepared from induction-melted solid and strength at high temperature. J Eur Ceram Soc. 2002;22:2621-5.

[11] Duong H, Wolfenstine J. Creep-behavior of fine-grained 2-phase Al_2O_3-$Y_3Al_5O_{12}$ materials. Mater Sci Eng A. 1993;172:173-9.

[12] Palmero P, Montanaro L. Thermal and mechanical-induced phase transformations during YAG and alumina-YAG syntheses. J Therm Anal Calorim. 2007;88:261-7.

[13] Young RA. The rietveld method. Oxford: Oxford Press; 1995. p. 5-21.

[14] Cheary RW, Coelho A. A fundamental parameters approach to X-ray line-profile fitting. J Appl Crystallogr. 1992;25:109-21.

[15] Neiman AY, Tkachenko EV. Conditions and macromechanism of the solid-phase synthesis of yttrium aluminates. Russ. J Inorg Chem. 1980;25:2340-5.

[16] Lima ES, Louro LHL, Costa CRC, de Campos JB, Costa CA. Microstructure of Al_2O_3/YAG eutectic composite. Brazilian Journal of Morphological Sciences, Supplement. 2005;316.

[17] Kong LB, Ma J, Huang H. Low temperature formation of yttrium aluminum garnet from oxides via a high-energy ball milling process. Mater Lett. 2002;56:344-8.

[18] Lima ES. Sinterização do SiC com adição do compósito Al_2O_3-YAG [DC thesis]. Brazil: Instituto Militar de Engenharia; 2006.

[19] Wen L, Sun X, Xiu Z. Synthesis of nanocrystalline yttria powder and fabrication of transparent YAG ceramics. J Eur Ceram Soc. 2004;24:2681-8.

[20] Li JG, Ikegami T, Lee JH, Mori T, Yajima Y. Co-precipitation synthesis and sintering of yttrium aluminum garnet (YAG) powders: The effect of precipitant. J Eur Ceram Soc. 2000;20: 2395-405.

[21] Tachiwaki T, Yoshinaka, M, Hirota, K, Ikegami T, Yamaguchi O. Novel synthesis of $Y_3Al_5O_{12}$ (YAG) leading to transparent ceramics. Sol St Comm. 2001;119:603-6.

[22] Li X, Liu H, Wang J, Zhang X, Cui H. Preparation and properties of YAG nano-sized powder from different precipitating agent. Opt Mater. 2004;25:407-12.

[23] Palmero P, Esnouf C. Phase and microstructural evolution of yttrium-doped nanocrystalline alumina: A contribution of advanced microscopy techniques. J Eur Ceram Soc. 2011;31: 507-16.

[24] Won CW, Nersisyan HH, Won HI. Efficient solid-state route for the preparation of spherical YAG: Ce phosphor particles. J Alloys Compd. 2011;509:2621-6.

[25] Hassanzadeh-Tabrizi SA, Taheri-Nassaj E. Compressibility and sinterability of Al_2O_3 – YAG nanocomposite powder synthesized by an aqueous sol – gel method. J Alloys Compd. 2010;506:640-4.